Contents

List of Figures

Sommario

La tesi descrive l'analisi effettuata su modelli rappresentanti gli arti superiori del corpo umano di un pilota di elicottero sottoposto a disturbi esterni.
In particolare, l'oggetto dell'indagine è l'interazione pilota-elicottero che può provocare un degrado delle prestazioni e delle caratteristiche di manovra del mezzo fino a causare la destabilizzazione del sistema.
Vengono distinte due classi principali di interazioni: quelle relative a un intervento volontario del pilota (PIO) e quelle relative a un suo intervento involontario (PAO).
Nel primo caso il pilota muove intenzionalmente un comando al fine di effettuare una qualche operazione, ma l'ingresso (*input*) è alterato da un'erronea percezione.
La determinazione di quali percezioni possono generare tali errori richiede un'indagine interdisciplinare, che supera i confini dell'ingegneria aerospaziale e sfocia nei settori della biomeccanica e della psicologia.
Come detto, il pilota può intervenire sui comandi di volo anche in maniera involontaria, in conseguenza di stimoli provenienti dall'esterno, come ad esempio a seguito della vibrazione del sedile o di altre parti della cabina di guida. Tali stimoli possono produrre un movimento non intenzionale della leva di comando, filtrato dalla dinamica passiva degli arti del pilota stesso.
Si è quindi partiti da un modello comprendente solo il braccio del pilota per poi arrivare ad uno più complesso, con l'introduzione di un modello di elicottero.
Nella prima parte vengono esaminate le dinamiche associate al sistema pilota-collettivo, tramite un modello biomeccanico dell'arto sinistro, sottoposto a diverse tipologie di disturbi.
Nella seconda parte oggetto dell'analisi è il braccio destro del pilota che governa il comando del ciclico.
In entrambi i casi vengono mostrati i risultati dell'analisi diretta sotto forma di risposte in frequenza.
Infine viene testato un modello multicorpo di elicottero, nello specifico il

BO105, nel quale sarà inserito il braccio sinistro, oggetto di studio nei capitoli precedenti, con il relativo comando, azionabile tramite cambiamento delle attivazioni muscolari.
Si è cercato di riprodurre il fenomeno del "vertical bounce", proprio di tutti gli elicotteri, consistente in un movimento verticale del mezzo, causato da un'oscillazione della leva di controllo introdotta involontariamente dal pilota.

Chapter 1

Summary

This thesis project represents the continuation of the previous work carried out by Ing. Andrea Zanoni[1], from which the model of left arm and its results of the inverse analysis were taken.
It is a part of a larger study on the possible causes of unintended and unexpected oscillations of the coupled system pilot-helicopter. Such fluctuations may lead to a divergent motions that are likely to cause serious accidents. There are two types of destabilization and participation of the pilot in the control loop:

- PIO: Pilot - Induced Oscillations;
- PAO: Pilot - Assisted Oscillations;

The first kind arises when the pilot introduces a phase lag or moves the controls in the wrong direction, possibly in response to misleading cues. This type of movement needs an active involvement of the pilot in the control loop, so if he releases the controls PIO will cease. So this destabilization is not always detrimental of flight safety.
The second kind sees the involuntary participation of the pilot in the control loop, and thus it is more related to pilot biomechanics and biodynamics, so heavily dependent from his body type, experience, and neuromuscular system characteristics.
There are a lot of work that try to explain how and why these oscillation arise and evolve ([4] and [5]).
A normal approach is to measure the displacements of control while the pilot is subject to a known vibration in order to reconstruct the transfer function that represents its impedance characteristics.
So, in this work the direct analysis of both the arms connected with collective lever and cyclic stick will be shown under different periodical disturbances.

Furthermore, the behaviour of the pilot coupled with an helicopter will be shown during some maneuvers.
Therefore, this thesis, and its possible future development, fits into this context with the assumption of being able to study the stability of the system with different types of pilots. In fact it is possible to change the height, the weight, the size of the limbs etc. etc. of the pilot to try a wide range of possibilities and, for each of them, studying the stability curves, understanding what leads to instability, and what are the physical limits within which the pilot should stay. It is clear that it is difficult to take into account the skill of the pilot, his reaction times and how he reacts to external stimuli.

Chapter 2

Introduction

At present, this part of the project is still at the already mentioned work made by Andrea Zanoni [1].
Thanks to this one, it was possible to define a general methodology able to estimate the mechanical impedance of the human arm in the control phase of a vehicle, using multibody techniques. This methodology is applicable to a wide range of geometries of the cockpit, pilots, biomechanical and physiological characteristics.

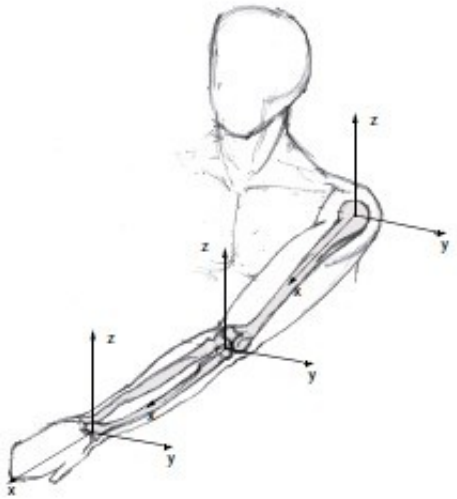

Figure 2.1: *Left arm (illustration courtesy of Chiara Contini)*

The bio-mechanical multibody model of the arm was realized by the general-purpose multibody software *MBDyn*, available under GNU GPL 2.1 open-source licence at *http://www.aero.polimi.it/mbdyn/*.
The goal of this work was achieved in three steps:

- a first kinematic analysis (with no gravity) useful to set correctly the model;
- an inverse analysis at all three levels, position, velocity and acceleration, with a procedure capable of resolving the redundancy at the first level. The quality of the solution is then checked constantly at the successive levels, by means of subsequent constrained optimizations. This analysis was able to derive the torques of shoulder, elbow, pronosupination and wrist that rise after the imposing a specific path to the hand;
- at the end an analytical approach has been developed to estimate the equivalent impedance characteristics of the upper limb.

2.1 Inverse analysis

In order to calculate the torque needed to perform a task or, equivalently, to follow a trajectory of the hand known in advance, the time histories of the positions, velocities and accelerations of each joint must be imposed in a problem of inverse dynamics.
The kinematics of the model is, however, under-constrained, because, by imposing the trajectory of the hand, a maximum of six movements can be prescribed through rehonomic constraints. The system therefore has infinite solutions equivalent, ie causing the same trajectory of the hand.
Since the hand can be considered as the end-effector of the system, the equivalence means also that the same task is reached.
As listed in the following section, there are four rigid bodies for a total of 24 degrees of freedom. To these are added the 17 equations of non-linear constraint representing the articular joints. These ones can be assembled into:

$$\Phi(q) = 0 \tag{2.1}$$

alongside to those, the rehonomic constraints prescribing the trajectory of the hand are:

$$\Psi(q) = q_h(t) \tag{2.2}$$

In a system completely determined, in which the number of constraints equals the number of degrees of freedom (n), the kinematics is often resolved at the level of the velocity by differentiating the last expression with

respect to time to obtain a linear system of n equations in n unknowns at each time instant:

$$[\varphi(\mathbf{q},t)]\,\dot{q} = \begin{bmatrix} \left[\Phi_{/q}\right] \\ \\ \left[\Psi_{/q}\dot{q}\right] \end{bmatrix} = \begin{bmatrix} 0 \\ \\ \dot{q}_h(t) \end{bmatrix} \tag{2.3}$$

2.2 Muscular activation

The muscular activation is a parameter between 0 and 1, which indicates how much the muscle is working during a certain action.
This indicator can be seen as the sum of two contributions, an intrinsic part and a reflective part. This distinction is easier to understand at the level of mechanical impedance, the first one is the part that comes from the viscoelastic characteristics of the muscle itself and it is the one that can be associated to the behavior of the muscle seen as elastic/damping element.
The second one comes from the voluntary or involuntary action of a person: is the part that derives from the characteristic of the muscle seen as an actuator.
The difference is that in the first case a part of implementation can be assigned only for the maintenance of a certain kinematic condition, while in the second case there is also a part of activation which depends on the desire of the person to pursue an objective.
For example, if the pilot simply rests his hand on a command, without doing anything, to maintain that position in front of an external disturbance, he is using only the non-reflective part of activation and therefore the command feels only the not-reflective part (passive) of the impedance. In the case where the pilot is actually trying to accomplish a goal, for example to maintain a certain height acting on the collective, the impedance felt by the command, and then the activation present in the muscles, will be the reflective one, which will usually produces an impedance from 10 to 20 times greater.

2.3 Ergonomic function

The model and the costraints were modeled in according to Pennestrí [6]. This work describes the three joint of the upper limb and the constraints

under which the system is subjected.
From the same paper the ergonomic function were taken and used to overcome the problem that arises from having too many equations of motion and too few constraint equations. For each joint, the author models the phisycal limits, that reduce the range of motion of the links, according to anatomical properties (Zatsiorsky [7]). He defines an ergonomic function $H(\alpha_i)$ with $i = 1, ..., 9$:

$$H(\alpha) = \sum w_i \frac{(\alpha_i - \alpha_{M_i})^4}{(\Delta\alpha_i)^4} \tag{2.4}$$

where α_i are the joints angles, w_i are the weighting coefficients and

$$\alpha_{M_i} = \frac{\alpha_{max} + \alpha_{min}}{2} \tag{2.5}$$

$$\Delta\alpha_{M_i} = \frac{\alpha_{max} - \alpha_{min}}{2} \tag{2.6}$$

The goal of this function will be discussed in the follow chapter.

2.4 Approximation of the neuromuscular system

From the literature, a quasi-stationary approximation of the activation originated from motor reflective impulses of the neuromuscular system has been taken and used in the direct analysis described in the following chapters.
The starting point for this controller comes from the work of Zanoni, Masarati, Quaranta [2], in which, to account for both the 'reflexive' both the 'intrinsic' part, the perturbation of the muscular forces is expressed as:

$$\delta\mathbf{f} = \mathbf{f}_{/\mathbf{l}}\delta\mathbf{l} + \mathbf{f}_{/\dot{\mathbf{l}}}\delta\dot{\mathbf{l}} + \mathbf{f}_{/\mathbf{a}}\delta\mathbf{a} \tag{2.7}$$

where the perturbation of activation, as a very preliminary approximation, is associated to the reflexive system by means of a simple proportionality relationship:

$$\delta\mathbf{a} = \mathbf{K}_p diag\left(\frac{1}{l_0}\right)\delta\mathbf{l} + \mathbf{K}_d diag\left(\frac{1}{V_0}\right)\delta\dot{\mathbf{l}} \tag{2.8}$$

where matrices $\mathbf{K}_p$ and $\mathbf{K}_d$ contain the proportional and derivative gains on the main diagonal, which essentially describes how the activation changes as a consequence of a position or velocity error. Thei diagonal values were taken from the literature and in particular from the work by Sybert Stroeve [3], and are respectively 0.8 and 0.03 (0.08 in these analysis).

$$\delta \mathbf{l} = \mathbf{l}_a - \mathbf{l}_d \tag{2.9}$$

$$\delta \dot{\mathbf{l}} = \dot{\mathbf{l}}_a - \dot{\mathbf{l}}_d \tag{2.10}$$

where $\mathbf{l}_a$ and $\dot{\mathbf{l}}_a$ are the actual length and elongation velocity, and $\mathbf{l}_d$ and $\dot{\mathbf{l}}_d$ are the desired ones.
So the activation considered in the direct analysis is:

$$\mathbf{a} = a_0 + \delta \mathbf{a} \tag{2.11}$$

where a_0 is the activation found thanks to the inverse analysis.

Chapter 3

Direct analysis of collective handle

3.1 The model

A four rigid bodies, seven degrees of freedom multibody model was designed for this analysis. It accounts for the motion of the humerus, radius, ulna and the hand, and the action of 25 muscles of the shoulder, arm and forearm, modeled as non linear viscoelastic elements that can be actuated. The joints can be summarized in:

- a spherical joint between the rest of the body and humerus (3 constraint equations);
- a revolute joint between humerus and ulna (5 constraint equations);
- a spherical joint between humerus and radius (3 constraint equations);
- a guide between ulna and radius (2 constraint equations);
- a universal joint between radius and hand (4 constraint equations).

So there are 17 constraint equations and 24 (4 bodies with 6 degrees of freedom each) generalized coordinates, which leads to 7 degrees-of-freedom. Introducing some driving constrains that can be added to joint equations in order to describe the desired movement of the hand and reduce the degree of freedom. In the proposed simulation the hand is constrained to the collective lever. This assumption, introduces other constraint equations leaving free less degree of freedom.
Anyway there are not enough equation to solve the kinematic problem.

For this reason the ergonomic function named previously is introducted like objective functions in order to find a solution, which satisfies the constraint equations and minimize these functions.
Then, a clamp joint connects the arm to the ground node at witch the required motion is applied.
There are several reference systems, one for each body, one for each muscle and many others used to help the construction of the model. So the one taken in consideration to impose the desired motion was the ground reference with the origin about in the coccyx, x directed forward, y to the left and, of course, z directed to upward.
This model is substantially the same of the one used for the inverse dynamic with some exceptions: the four ergonomic springs and the four joints previously used to obtain the torques were deleted and as well as the imposed motion applied to the hand. Furthermore for what concern the *MBDyn* software, the problem become an *initial value problem*.
A simple PD-controller was added to hold the correct position. Thus it was necessary selecting the target position and, before start this direct analysis, a preliminary inverse one was required in order to obtain the right activations and lengths that each muscle had in this position and that must be maintained during the process.
Therefore the first step was to develop this analysis with the arm that followed a path that brought the handle to the desired excursion (50% of the maximal one in this case). Then the correspondent activations and lengths were found thanks to a *Matlab* script and saved for the new direct model.

3.2 First direct analysis

A first analysis, common to all the other ones, was made with no external force or noise. The only load applied to the arm was the gravity, because, like previously said, in the preliminary kinematic analysis there was no gravity force so its introduction in this step can already be seen like a sort of disturbance. It was necessary obtaining the graphic of the response of the system under the gravity load, applied with a cosine law, to understand in how much time the perturbation due to gravity fades away.
Like it can be seen in figure 3.1,the time required to bring the arm in the initial position is too long respect to the test time, so there was the need for more attempts with different, and major, $\mathbf{K}_d$. That can be done because sustaining gravity is not the goal of this analysis but just the initial

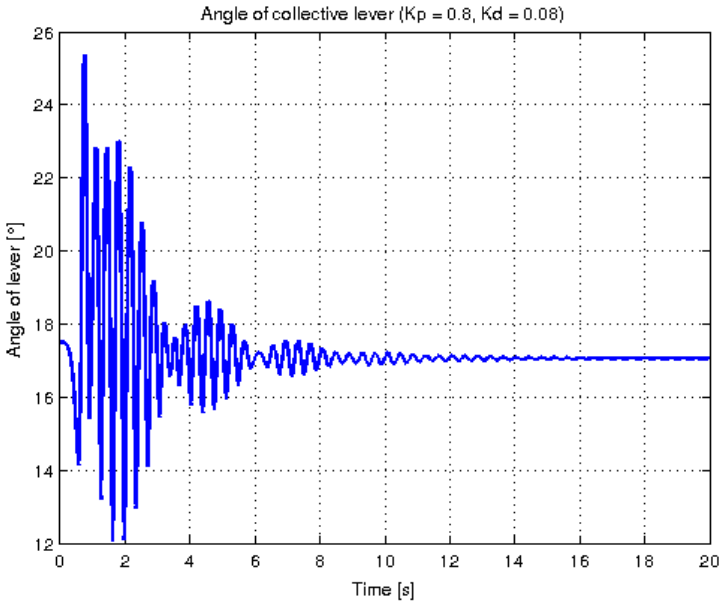

Figure 3.1: *Angle of collective lever*

condition. The figure 3.2 shows the response of the system at $K_d = 2.88$. The value reached by the system after the perturbation is 17.5078 and the error on the position is only the 0.04%.
The time required to bring the system in the initial position is greatly shorter then before so, for the next tries, K_d will be maintained at this value for the first seconds of test.

3.3 Imposed motion along the z direction

3.3.1 Periodical displacement

In this phase of work the arm was subjected to a periodical displacement form 1 to 8 Hz.
The input signal was chosen in order to have an acceleration like:

$$\ddot{z} = Asin\,(\omega t) \tag{3.1}$$

so the displacement was taken like:

$$z = -\frac{A}{\omega^2} sin\,(\omega t) \tag{3.2}$$

The amplitude of displacement at 1 Hz is 0.0101 m (figure 3.3) and, like

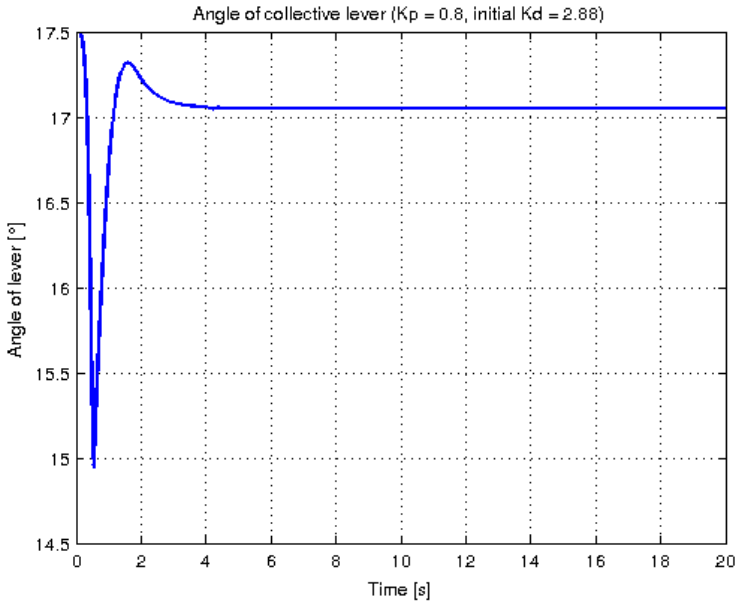

Figure 3.2: *Angle of collective lever*

it can be seen from the plot, it starts after that the system has reached the equilibrium point.

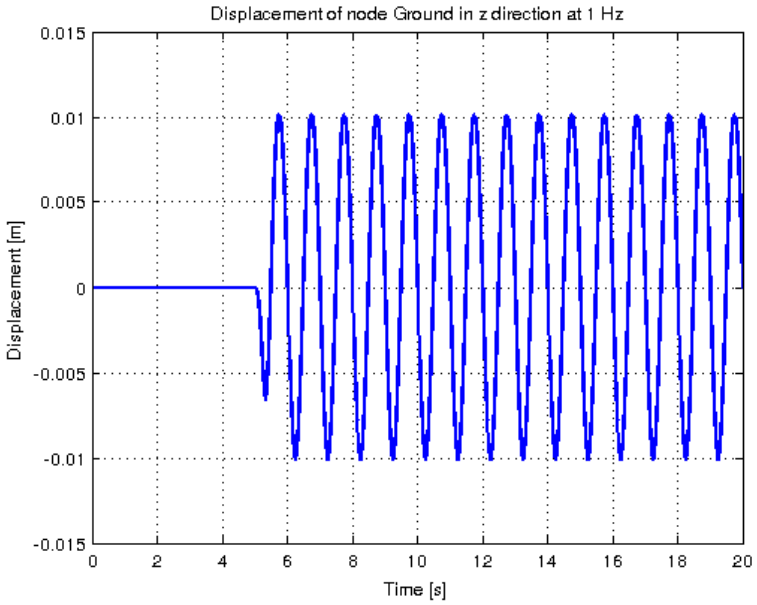

Figure 3.3: *Displacement at 1 Hz*

The response of the system is as expected periodical with a certain amplitude and frequency equal at 1 Hz.
The peak frequency detected during the experimental tests in Liverpool was around 3 Hz, and the same result was found by these numerical tests. So at this frequency the system shows the greatest variation of angle of lever.
The follow pictures show the response of the arm under an acceleration equal in amplitude but with different frequency (figure 3.4 and 3.5):

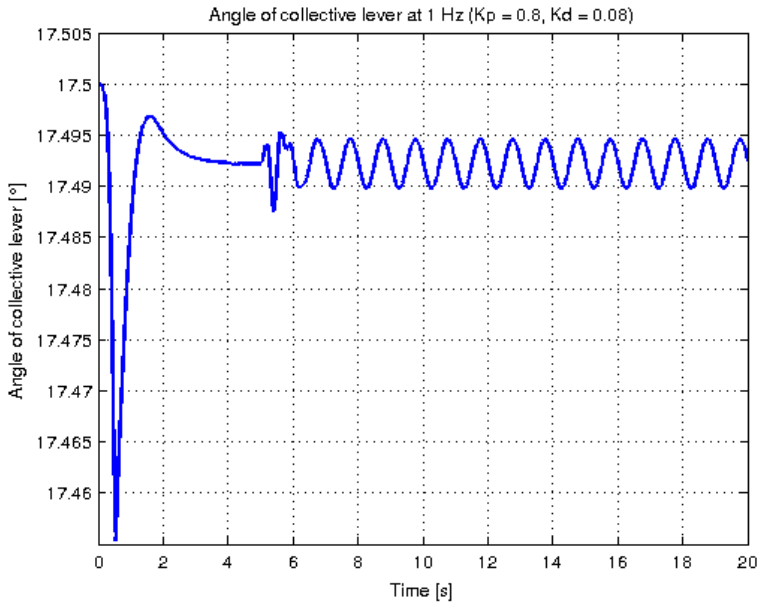

Figure 3.4: *Angle of collective lever at 1 Hz*

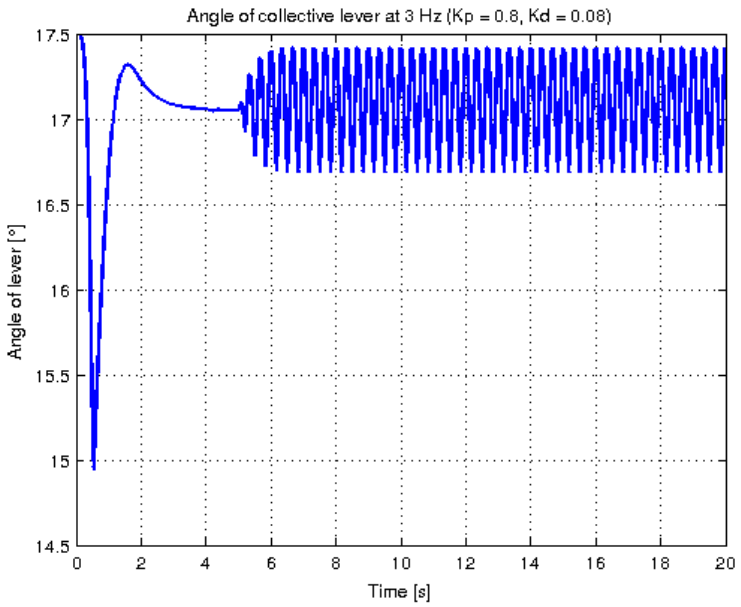

Figure 3.5: *Angle of collective lever at 3 Hz*

It can be seen how the system responds with a short transient (about a second) before going definitively to scheme.

3.3.2 Frequency response

Doing various tests at different frequencies, it was possible to gain the plot of the module and phase of the function transfer that highlights the correct peak at 3 Hz (figure 3.6).
Other attempts have been made with different K_p to see how much the position of the peak changes. In figure 3.7 and 3.8 the function trasfer is plotted with K_p equal respectevly 0.5 and 1.5. Like it can be seen the peak goes backward (about 2.5 Hz) when $K_p = 0.5$ and forward when $K_p = 1.5$.

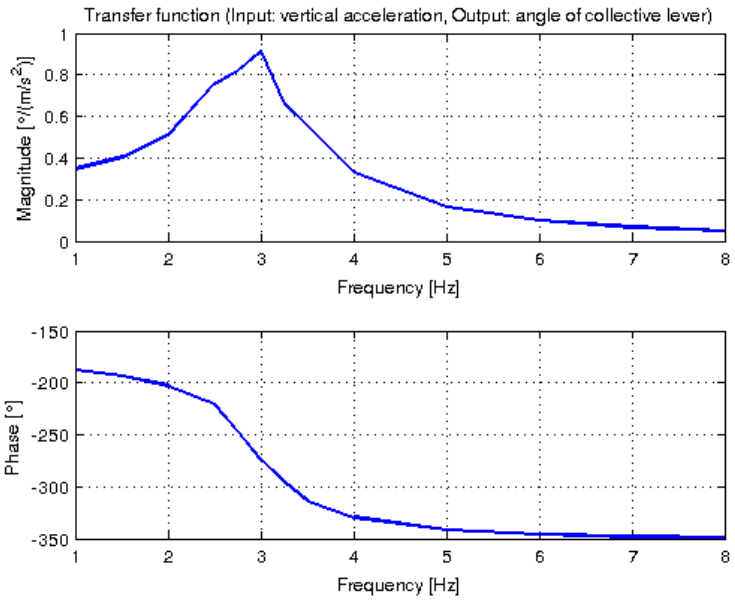

Figure 3.6: *Frequency response with* $K_p = 0.8$ *and* $k_d = 0.08$

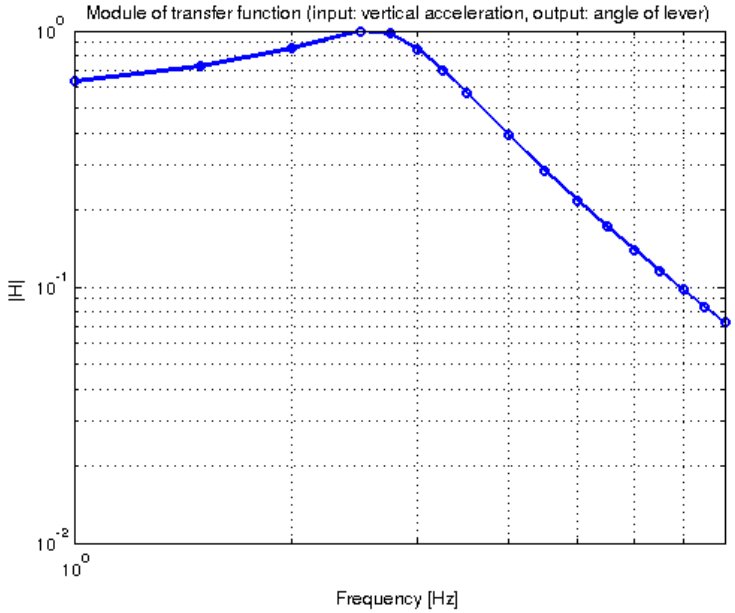

Figure 3.7: *Frequency response with* $K_p = 0.5$ *and* $k_d = 0.08$

From the literature it is provided a comparison with other experiments, in particular in the work of John R. Mayo[9] is taken into account the analysis of collective subjected to vertical vibrations.

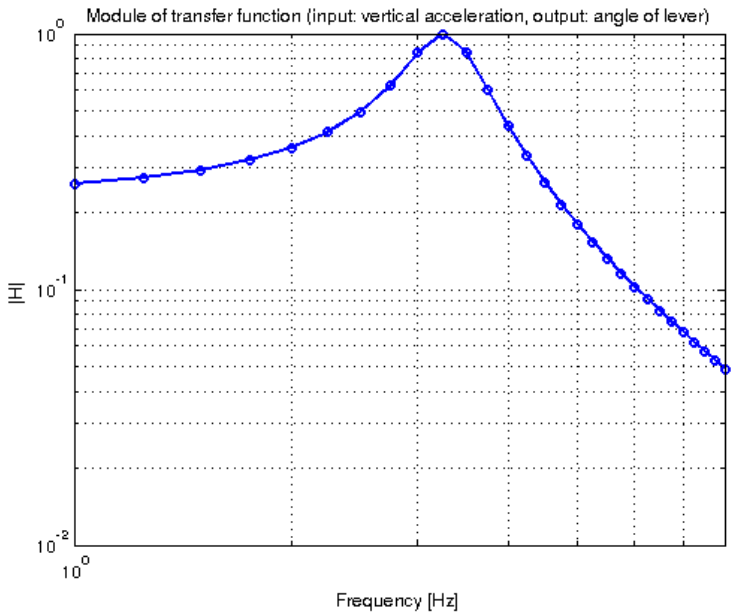

Figure 3.8: *Frequency response with* $K_p = 1.5$ *and* $k_d = 0.08$

His analysis provides a transfer function with input the absolute acceleration of the seat and with output the absolute acceleration of the lever. The results presented below have been revised as suggested in [11] to transform the output into a relative rotation of the command.
The transfer function proposed by Mayo is:

$$H_{abs}(s) = \frac{5.19s + 452.3}{s^2 + 13.7s + 452.3} \tag{3.3}$$

To transforme it into the (relative) rotation of the collective bar as a function of the vertical acceleration of the seat it is necessary to carry out some steps.
The relative acceleration, namely the acceleration of the pilot's hand with respect to the acceleration of the cockpit is:

$$H_{rel}(s) = H_{abs}(s) - 1 \tag{3.4}$$

The rotation of the bar is obtained by dividing the relative acceleration by the distance L between the collective bar hinge and the point where the pilot grabs the stick, and by integrating twice:

$$\Delta\theta(s) = \frac{1}{s^2}\frac{1}{L}(H_{abs}(s) - 1)a(s) \tag{3.5}$$

where $a(s)$ is the imposed acceleration.
The presence of two integrators in equation yields a drifting behavior when $s \to 0$. What this transfer function is missing is the fact that the pilot's active behavior will compensate any low-frequency change of collective inceptor position as soon as it is adequately detected. To account for this, the functions are high-pass filtered by turning the integrator poles $\frac{1}{s^2}$ into stable real poles α_1, α_2 close to zero ($\alpha_i < 0$), namely:

$$\Delta\theta(s) = \frac{1}{(s-\alpha_1)(s-\alpha_2)} \frac{1}{L} (H_{abs}(s) - 1) a(s) \tag{3.6}$$

In figure 3.9 this transformation is applied bringing only a single pole of the integrator at 1 Hz.

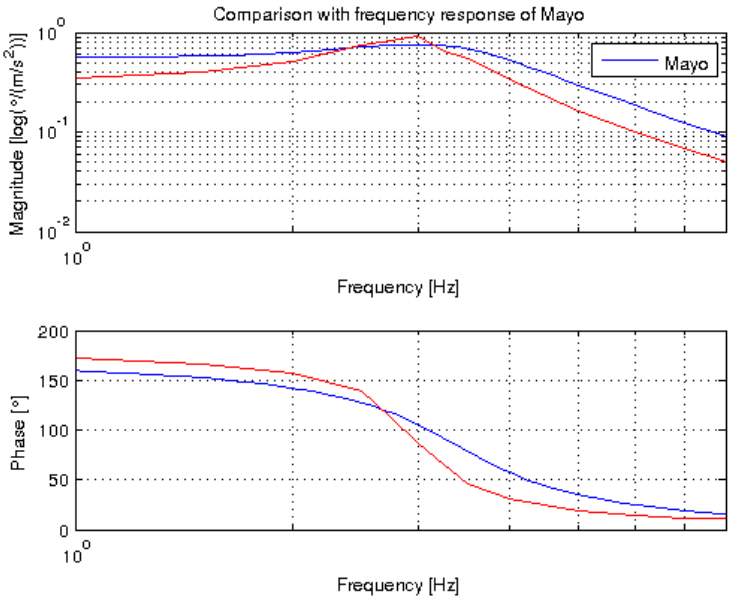

Figure 3.9: *Comparison with Mayo's frequency response*

3.4 Imposed motion along x and y direction

It's interesting to know what kind of displacement brings the greatest oscillations on the response of the system. So the same tests were made also along the other two axes to see how much the angle of lever is influenced by vibrations that come from all the directions.

It's important to remember that the handle can't move along y axis because the only rotation allowed to the collective lever is about this axis. As expected, the trasversal vibration have less influence on the dynamics of the lever becouse. The frequency peak has remained about 3 Hz (figure 3.10) and in 3.11 it can be seen the response of the system at such frequency.
On the contrary, the system is found to be more sensitive to oscillations along the x direction. In this case the peak moved to 2.5 Hz (figure 3.12) and in figure 3.13 is plotted its response.

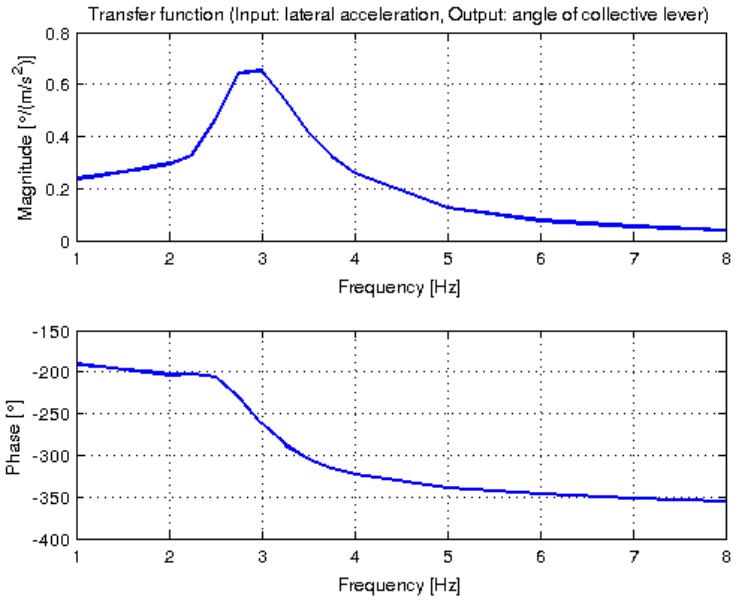

Figure 3.10: *Frequency response with vibration along y axis*

Lastly it is useful to compare the three graphs of the modules of the transfer functions, with the relative phases, in a single plot.
The result is shown in figure 3.14: the imposed displacement along x axis and the angle of the lever working out of phase by 180° at low frequencies. In resonance the phase decreases by 90° and, as the frequencies grow, input and output are increasingly working in phase. The behavior of the phase for the other two directions of displacement is about the same for movements along y and z.
Speech reverse is true if as input is taken the acceleration (figure 3.15), being this offset by 180° with respect to the imposed displacement, the phase shift at low frequanze is about zero, that is, by accelerating the system forward (positive direction), for example, the lever rotates bringing the handle back and then increasing its angle.

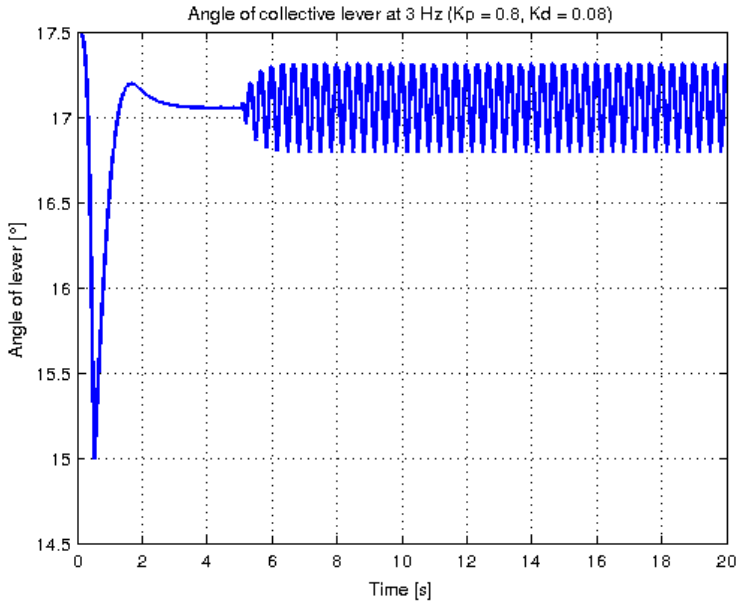

Figure 3.11: *Angle of collective lever at 3 Hz*

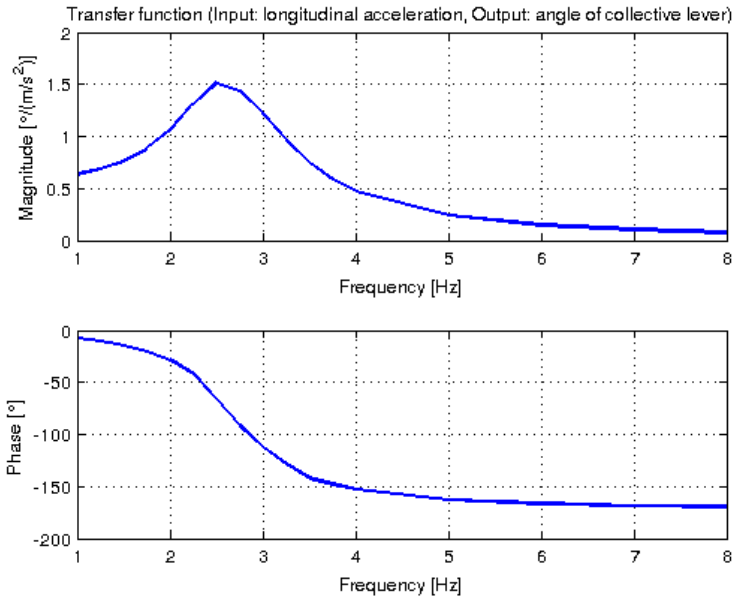

Figure 3.12: *Frequency response with vibration along x axis*

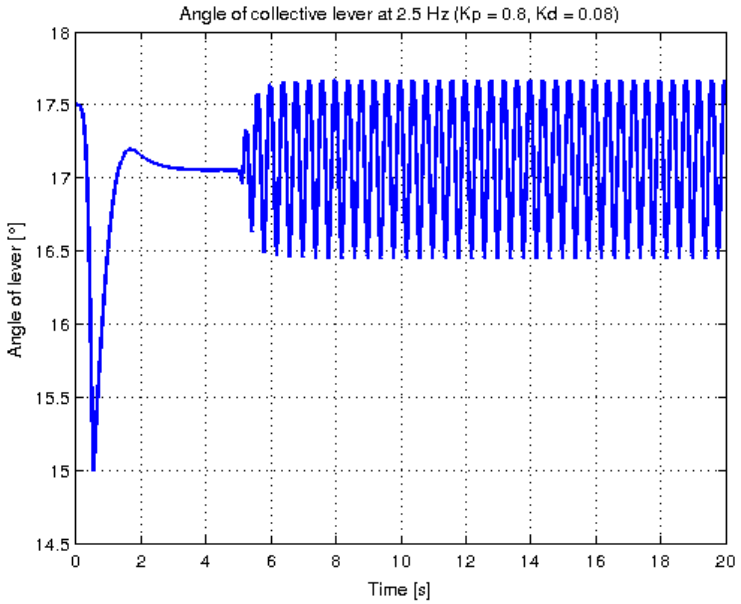

Figure 3.13: *Angle of collective lever at 2.5 Hz*

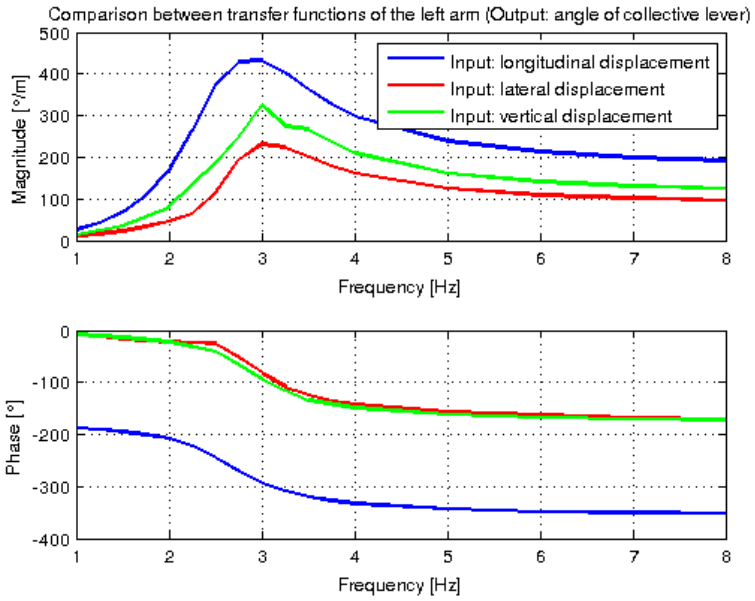

Figure 3.14: *Compare between frequency response (input: displacement)*

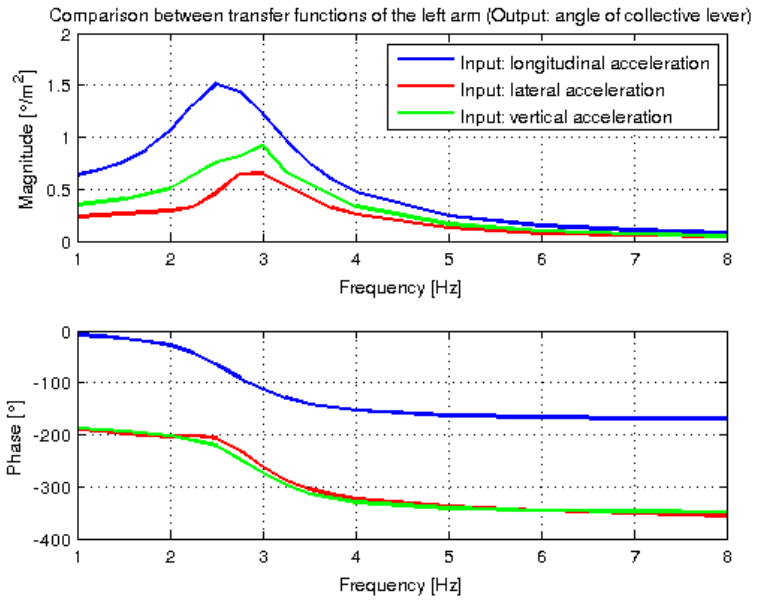

Figure 3.15: *Compare between frequency response (input: acceleration)*

3.5 Imposed motion about pitch axis

Further tests were conducted to show the behavior of the system under rotational vibration about the pitch axis, ie about the axis that, given the characteristics of the collective lever, more influence its behavior.
In the two following figures the module and the phase of the transfer function is shown with input in the first one, an sinusoidal acceleration about the y axis, while in the second one the relative sinusoidal rotation. For both figures the output is the angle of the collective.
It is useful to show a comparison with the frequency response relating to an acceleration about an axis which is expected much less influential on the command. In the figure this comparison is shown with the acceleration about the rolling axis.
As expected the module of the transfer function of the acceleration about x axis is much lower (3.18).

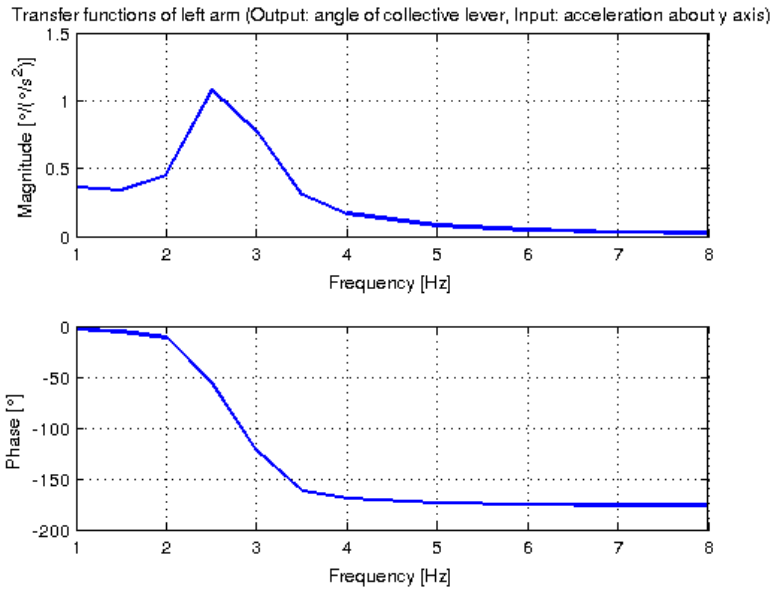

Figure 3.16: *Frequency response (input: acceleration about y axis)*

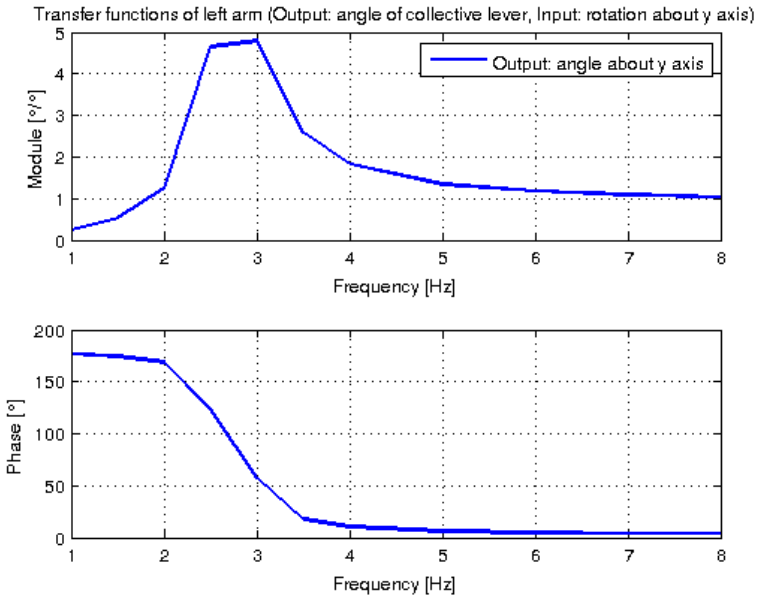

Figure 3.17: *Frequency response (input: rotation about y axis)*

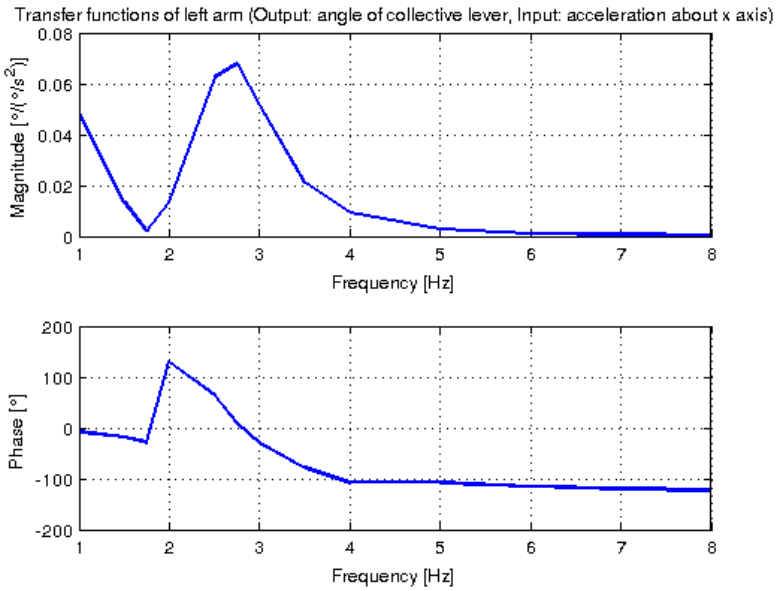

Figure 3.18: *Frequency response (input: acceleration about x axis)*

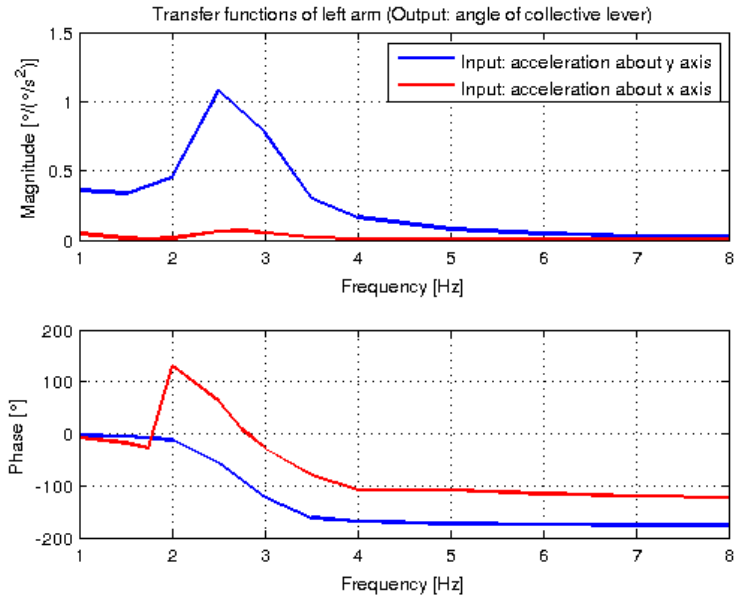

Figure 3.19: *Compare between frequency response (input: acceleration)*

Chapter 4

Analysis of cyclic stick

The next phase of work will focus on the right arm of the pilot and therefore on the cyclic stick.
This command is the most sophisticated and the most delicate among the controls of a helicopter. It is called the cyclic since it causes a cyclical variation of the angle of attack of the blades. That is, depending on the position in which these will be found during their rotation of 360° about the rotor, their angle of attack will undergo a change of slope equal for all the blades that will transit at that particular point. The result is to modify the lift generated by each single blade and thus to tilt the disc rotor in a given direction. It serves to optimize the propulsion, and in particular, to appropriately distribute the thrust in order to allow variations of trim and the displacement of the helicopter.

4.1 The model

The model of the arm used for the analysis of the cyclic stick is substantially the same as that one used for the anlysis of the left arm mirrored with respect to the x-z plane.
A different need to be done with regard to the type of the control lever. The cyclic stick is at $y = 0$ passing between the legs of the pilot and is subject to different kinematic constraints, the lever has the possibility to rotate both about the y axis, as the lever of the collective, and about the x axis. Then the only rotation prevented, is about the z axis.
Also this command has been equipped with mass, stiffness and damping, in order to best simulate the behavior of the real command that wants to perceive the driver the feeling of how he is moving the lever from its neutral position.
At least, it must be considered that in this model there is not the simul-

taneous presence of both arms, because, lacking the model of the chest, these ones are clamped to the seat and therefore it is not possible to combine the effect that one arm has on the other because it would act as two distinct parts.

4.1.1 The stick lever

Lacking the direct data of mass, stiffness and damping relative to the control lever, it was chosen to follow an alternative route.
It was to develop a simple dynamic model with kinematics described by the imposed displacement of the base and the rotation of the lever.
The equation that is obtained (in Laplace) is:

$$\left(Js^2 + Rs + K\right)\Theta = -mbs_2X \tag{4.1}$$

where J is the moment of inertia relative to the hinge of the lever, R the relative damping, K the stiffness of the command, Θ the rotation of the lever about the y axis, m its mass, b the position of the center of gravity along the z axis and X the imposed displacement.
K can be deduced from the results obtained during the ARISTOTEL biodynamic test campaign aimed at the characterization of the cockpit inceptors and from its relative sheet of laboratory of G. Quaranta "Identification of inceptor characteristics of UoL Bibby flight" which also describes the characteristics of the transfer function found. Thanks to these ones and the two complex conjugate poles $p = -14.2404 \pm 18.7329i = \sigma + i\omega$ it has been possible to obtain the missing data:

$$\omega = \left(\sqrt{1-\xi^2}\right)\omega_0 \tag{4.2}$$

$$\sigma = -\xi\omega_0 \tag{4.3}$$

and so

$$\omega_0 = \sqrt{\omega^2 + \sigma^2} \tag{4.4}$$

from which it is immediate to obtain:

$$J = \frac{K}{\omega_0}^2 \tag{4.5}$$

$$R = 2\xi\omega_0 J \tag{4.6}$$

If it writes the acceleration of the stick as the second derivative of $Y = X + L\Theta$, with L the length of the lever, replacing it in the equation of motion, it leads to the transfer function:

$$\frac{Y}{X} = 1 - \frac{mbLs^2}{Js^2 + Rs + K} \tag{4.7}$$

Obtaining the ratio input outputs from the graphs of the transfer function in the mentioned work of G. Quaranta, it was possible to find the value of mb.
For analytical purposes, it is not important to know the correct value of mass and center of gravity but only their product. Then it was sets a height of the center of gravity equal to $0.25m$ and the mass of the lever is found to be $4.2kg$.

4.2 Kinematic analysis

The first step of this phase of the project was a preliminary analysis to bring the arm from the initial position and move it until it reaches the control lever.
Throughout the analysis, as was done for the left arm, there is not the presence of gravity.
The final position the hand will be used as start position for the following analysis.
In figure 4.1(where is plotted the z component of the hand) it is possible to observe how the arm, starting from a position lying forward, initially flexes the elbow, causing a raising of the hand, and subsequently, by turning the shoulder, the hand falls and reaches the lever.

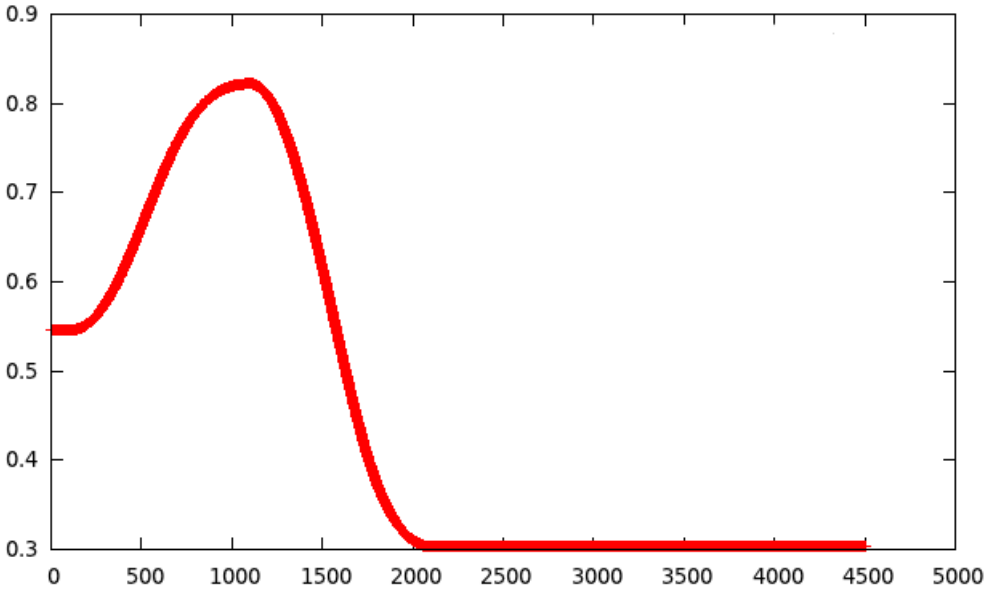

Figure 4.1: *Hand movement along the z axis*

4.3 Inverse analysis

As done for the left arm, also in this case it was necessary to perform an inverse dynamics analysis in order to calculate the activations that each muscle needs to maintain the lever in a given position.
Unlike the collective, where the movement of the lever was imposed by changing the orientation of the hinge constraint, in this case the procedure was a bit more laborious, because, having the cyclic stick two degrees of rotational freedom and not only one, the axis of rotation can be varied continuously.
A new node, free to slide along the axis of the lever, has been inserted in the model at the knot of the grip. The orientation of the latter one was bound to the node "ground" as well as its z coordinate so that, by imposing a shift, this could preserve the orientation of its reference system and, with simultaneous, slide freely along the lever as this ona will get up or down.
To derive the activations it was required of a motion that it needed both of the degrees of freedom available, so a shift command of the diagonals with return to the initial position. Once stopped its stroke, it has been possible to obtain the muscolar activations needed to maintain the command in

position using the same *Matlab* script used for the lef arm.
In figure 4.2, it is possible to see how the hand attached to the lever moves towards, along the x axis, and then return back to its initial position.

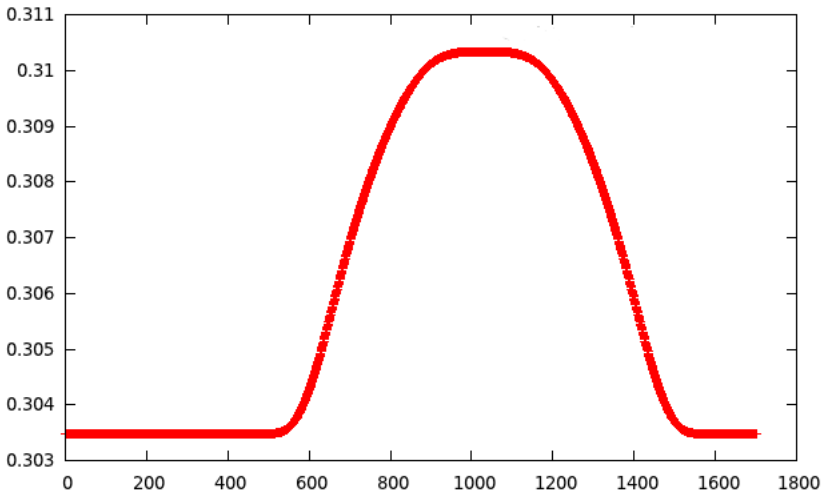

Figure 4.2: *Hand movement along the x axis during the inverse analysis*

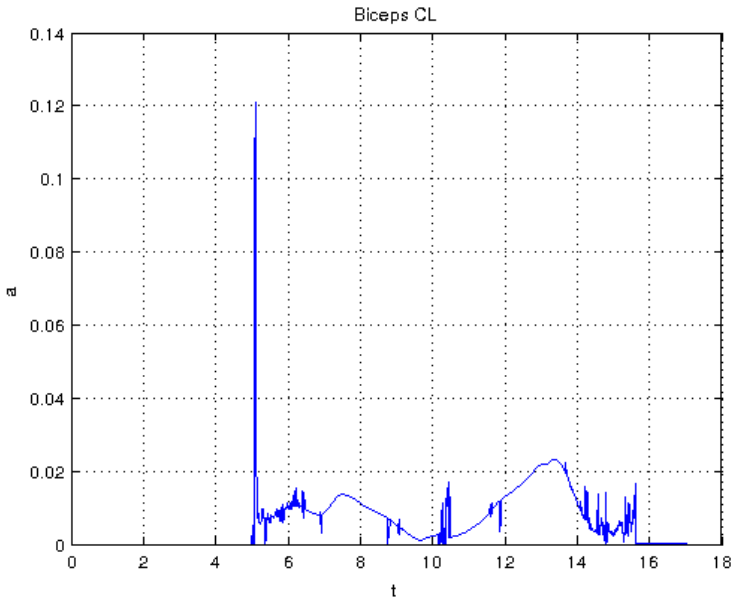

Figure 4.3: *Bicipite activation during the test*

The graph in figure 4.3 shows the evolution of the activation of the biceps during the test. As can be seen, there is a peak when the imposed motion

begins. At the end of stroke this one returns to almost zero and then up again when the lever moves backd. At the end of test the activation settles on a very low value since the muscle has only the task of maintaining the position counteracting gravity.
The non-symmetry of the two humps of the graph comes from the fact that pushing the lever forward triceps and shoulder are mainly activated, on the contrary, by pulling the biceps the biceps is more involved.

4.4 Direct analysis

Obtained activations, it is now possible to start the same direct analysis conducted on the left arm: a vibrational movement imposed along each direction and about each axis.
Unlike the previous case where the translation along the y-axis was little influence due to the constraints, with the right arm it assumes a greater importance as free to move in that direction. The translational motion in z is instead that one which in this case presents a greater decoupling between input and output, that is no longer the only rotation about y axis but also about x.
The controller put into effect to maintain the lever in the initial position is the same as described in chapter 3.2 because it is assumed that there is no difference between the muscles of the two arms.
It should be remembered that, even when it concerns lever cyclic tests, the starting position was taken from the final position of the static test, then without the gravity that will be added at the beginning of this test causing the transient already seen in the study of lever the collective. To avoid that the introduction of gravity would compromise the success of the test a method, similar to that used on the left arm but with times of transient slightly longer and higher coefficients K_d, was used. Set the time required to deplete this transient, it was therefore possible to complete the necessary tests.

4.4.1 Imposed motion along x direction - Results

The first two figures 4.4 and 4.5, show the transfer functions with the input vibrational motion imposed along the axis x and the output angle about the x-axis and y-axis respectively.
It can be seen, unlike the collective lever, the peak is lowered, reaching a frequency around 1 Hz (1.25 Hz for rotation about x and 1 Hz for rotation about y)

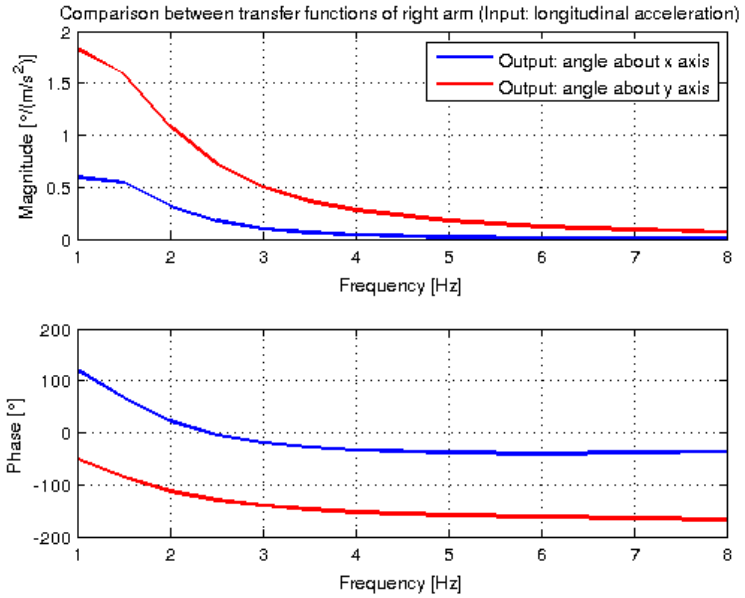

Figure 4.4: *Comparison between transfer functions (Input: acceleration)*

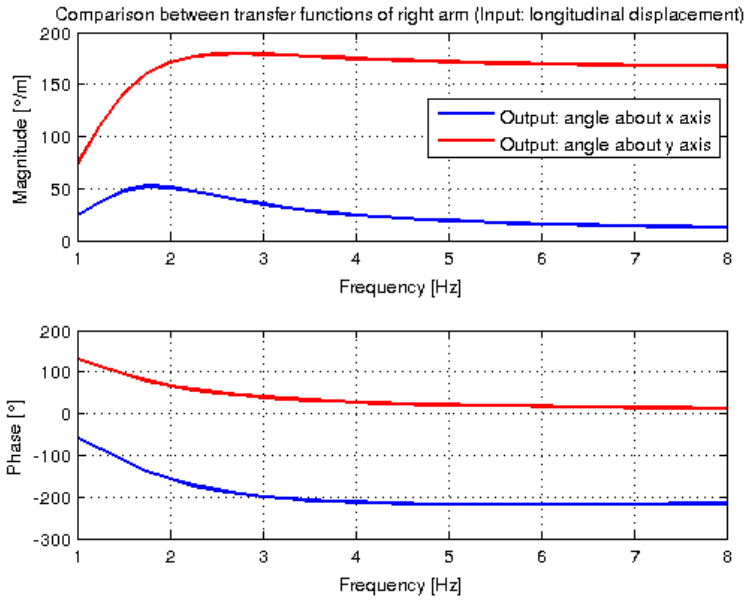

Figure 4.5: *Comparison between transfer functions (Input: displacement)*

4.4.2 Imposed motion along y direction - Results

In figure 4.6 the form of the transfer function relating to the acceleration around the y axis is plotted together with the relative phase. The frequanze peak is at 1 Hz for both rotations, while switch to 1.75 Hz for rotation about y axis and 2.75 Hz for rotations about x axis (fig. 4.7).
As expected the rotation around the x axis is much greater than the one about the axis y.
Even for the lever of cyclic, a comparison is available in the literature in the article by Tom Parham jr., who has analyzed the command subjected to lateral acceleration.
In the figure is plotted the comparison between the two analyzes. Unlike the model presented here, the y-axis used by Parham has an opposite positive direction, then the phase was shifted by 180°to make the comparison more similar and re-establishing equality of the axes (fig.4.8).

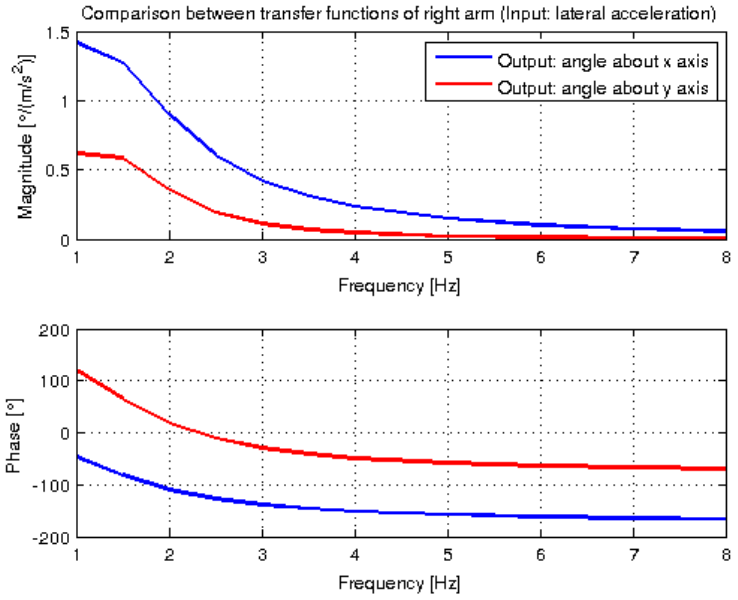

Figure 4.6: *Comparison between transfer functions (Input: acceleration)*

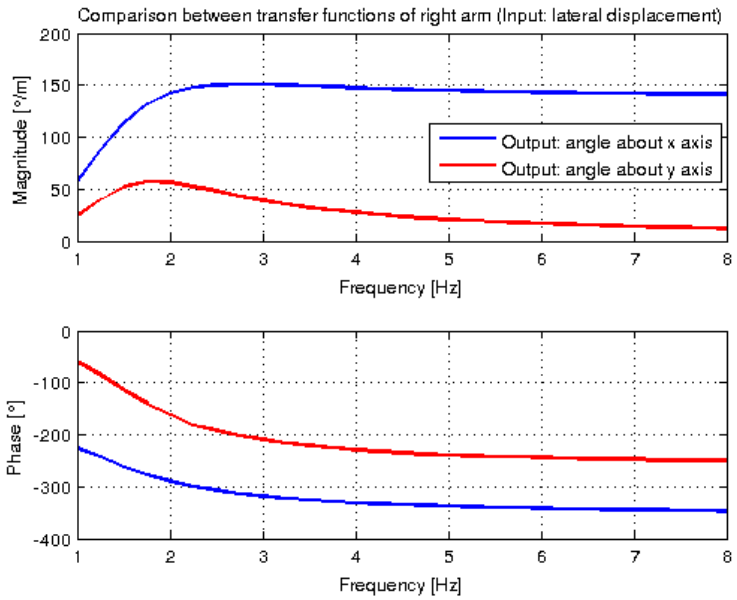

Figure 4.7: *Comparison between transfer functions (Input: displacement)*

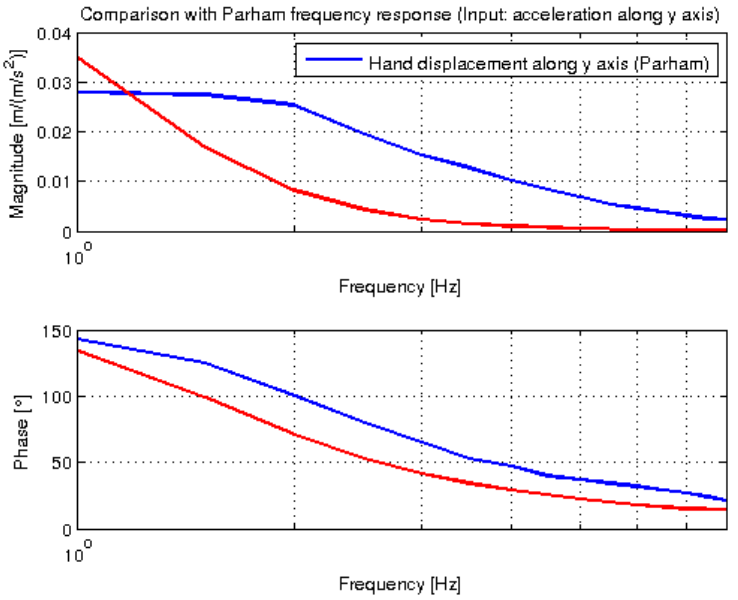

Figure 4.8: *Comparison with Parham's frequency response*

4.4.3 Imposed motion along z direction - Results

Among the rotations around the three axes, that around the z axis is definitely less influential on rotations of the command of the cyclic given the constraints to which it is subjected.
The results of the test input with a rotation about this axis are shown in figures where you can clearly see that the module of both functions and much smaller than aidue previous cases.

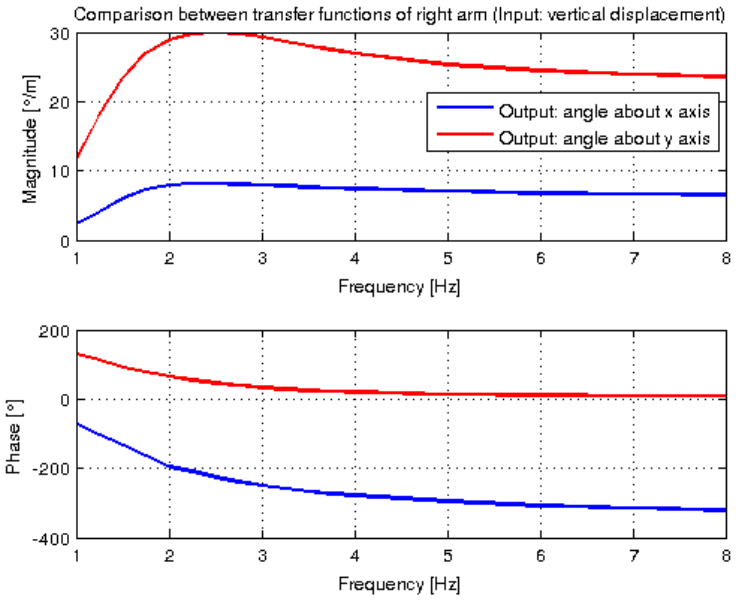

Figure 4.9: *Comparison between transfer functions (Input: displacement)*

4.4.4 Imposed motion about pitch and roll axes - Results

Unlike the collective, the command of the cyclic is influenced by rotational disturbances both about the pitch axis and about the roll axis.
The expected behavior from these tests is a greater influence on the angle of the collective about which the system is moving. The graphs in figure 4.10 and 4.11 confirm expectations and in particular show the transfer functions of the system subject to angular accelerations about both axes.

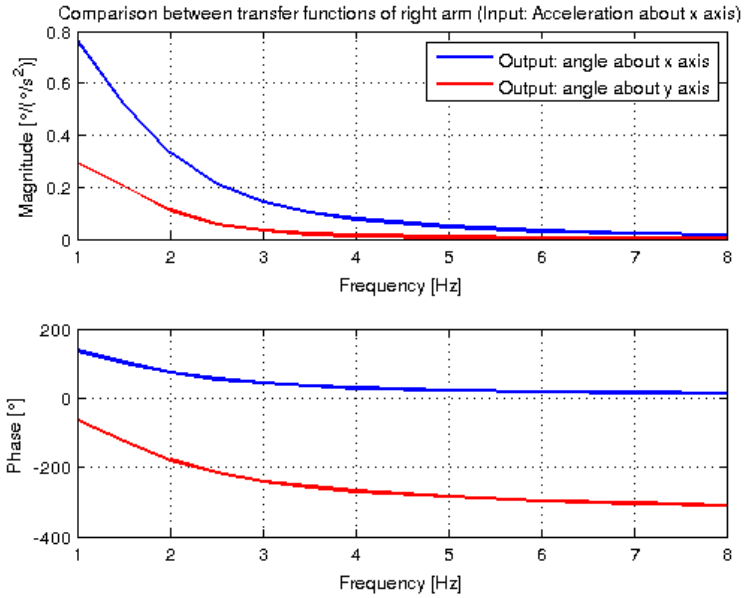

Figure 4.10: *Comparison between transfer functions (Input: acceleration about x axis)*

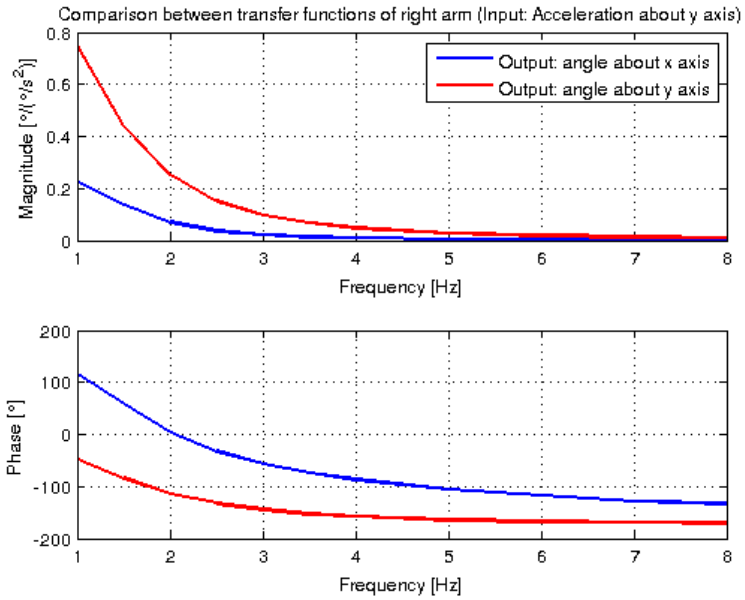

Figure 4.11: *Comparison between transfer functions (Input: acceleration about y axis)*

Chapter 5

Helicopter

As mentioned in the introduction, the last step consists in the tests of the coupled system-pilot helicopter. The helicopter selected is the BO105, not because it particularly subject to the type of instability studied, but because it is representative of the average tonnage models and all data necessary for the aeroelastic modeling are public.
The behavior of the system will be shown under different types of disturbances in order to understand which are the disturbances and which amplitude they must have to lead to instability.

5.1 The model

The BO105 helicopter has been implemented. Its structural dynamics are modeled using the free generic multibody solver *MBDyn*, developed by the aeroservoelasticity and structural dynamics research group of the 'Dipartimento di Ingegneria Aerospaziale', Politecnico di Milano.
The approach is quite general: the resolver MSD can directly manage many aspects of the problem, including aeroelasticity itself, although the way to manage the aerodynamics built into the program is limited to Blade Element/Momentum Theory (BE/MT), but it is also possible to delegate the fluiddynamic part to external solvers.
However, an efficient and accurate solver for the rotor aerodynamic, able to deal with large aeroservoelastic analysis required by RPC, is not available internally. Consequently, in this model, the aerodynamics is delegated to an external solver.
The structural model consists of the main rotor and the cell. The rotor is modeled using the approach multibody: constraints kinematically exact, applied by means of Lagrange multipliers, describe the relative motion between the rigid bodies which constitute the hub, the bearings of the

blades and the pitch control mechanism, while the dynamic structure is treated by linear finite element (FE) beam elements based on an original finite volume (FV) formulation, and concentrated masses.

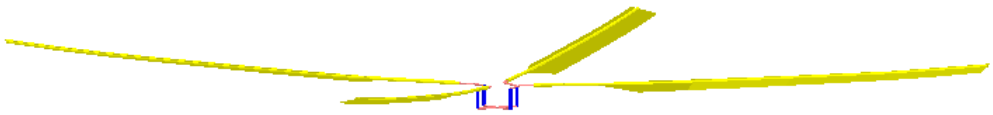

Figure 5.1: *Sketch of the main rotor*

The mass of the rotor was subsequently removed from the matrix of modal mass since the mass of the rotor is already provided by the multibody model of the rotor.
The interface between the CMS and the MSD domain model takes place at selected points, including the fixing points of the main rotor and tail rotor (although the tail rotor is approximated by a lumped force) and the seats of the pilot and co-pilot. The main rotor is connected to the cell by a revolute joint that imposes the relative angular velocity.
Although a complete model of free-flying helicopter, including the tail rotor has been developed for the purposes of this study, the overall motion of the helicopter as a rigid body is selectively constrained to respect the desired flight condition. Only the degrees of freedom which are important for each specific analysis are allowed.
For more in-depth analysis of the model, which also includes the aerodynamics, it is possible to make reference to some previous work on the same model ([11], [12] and [13]).
In addition to this model, has been inserted in place of the pilot, represented by a simple transfer function, the model of the left arm seen in the previous chapters.
A further modification to the model was performed on the control mode of the collective lever. Initially, the pitch was changed by acting, via a "drive caller", directly on the plate of the collective changing its inclination. Now it is the pilot, with a prescribed time history of muscle activations, raises or lowers the lever cyclic commanding directly the plate.

5.2 Perturbation of collective lever

The starting condition during the tests performed is that of *hover*, ie with the helicopter to stand still in the air develops a thrust equal to the force

of gravity applied to its mass.
The first test described involves a change in the corner of Collective generated by an upward movement of the lever and a speedy return to its original position.
Activations required to provide this movement have been obtained with the model used for the direct analysis. A movement of the lever has been imposed downwards. The arm, forced by the constraints to follow it, lowers itself but responds with an increase of muscle activations trying to counter the movement and trying to return the lever to its original position.
To these ones were subtracted the activations necessary to maintain the lever in its initial position obtaining the Δa required to move the lever of the same quantity of the test but in the opposite direction, and then upwards.
The test begins with the helicopter constrained. After one second of test the joint that keeps it fixed disappears and initially the helicopter loses altitude and then recover it through the control imposed on the arm. The decline in altitude is due to the usual problem of the arm that has to adapt itself to gravity.

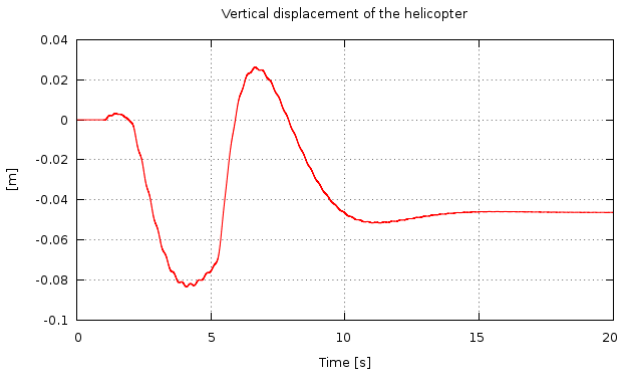

Figure 5.2: *Vertical displacement of the center of gravity of rotorcraft*

The real test begins after 5 seconds, at this moment, the "drive caller", that changes the muscle activations by a required amount, turns on making a first increase of activation turning the lever up and then restore these ones to their default value returning the lever to its initial position.
In figure 5.2 the vertical displacement of the helicopter is shown and it is possible to see how this one afetr one second of test loses the clamp that kept him still and undergoes a transition due to fluctuations of the arm

connected to the collective caused by gravity. As mentioned before, after 5 seconds there is a disturbance of the collective and the helicopter go up and then down settling to a certain altitude. The two figures below show the vertical acceleration of the center of gravity and the time history of the angle of the collective lever.
As expected the acceleration presents a oscillatory behavior given the type of movement imposed, with a positive peak at 5 seconds, ie at the moment in which the pilot increases the pitch angle of the blades.
Consequently, in the graph in figure 5.4 it can be seen the disturbance given to the collective at $t = 5s$.

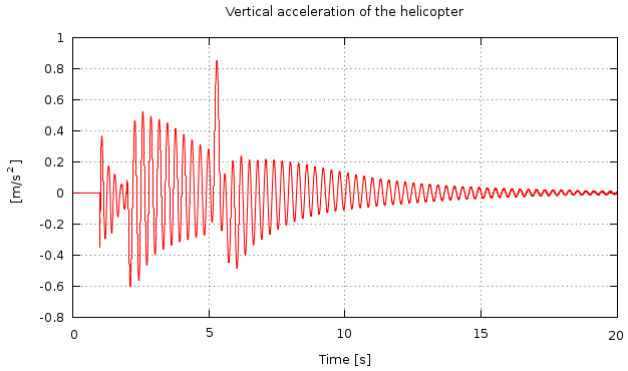

Figure 5.3: *Vertical acceleration of the center of gravity of rotorcraft*

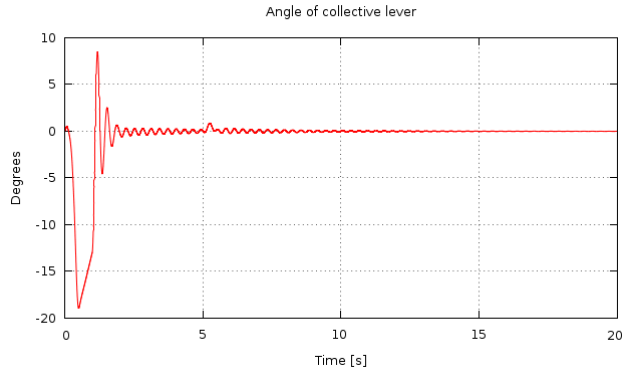

Figure 5.4: *Angle of collective lever*

In the last graph (figure 5.5) is present the displacement of the swash plate. As it can be seen, at the moment of disturbance there is a peak

downwards, this is because the pitch-link is placed behind the blade and so the plate must descend to increase the pitch of this one.

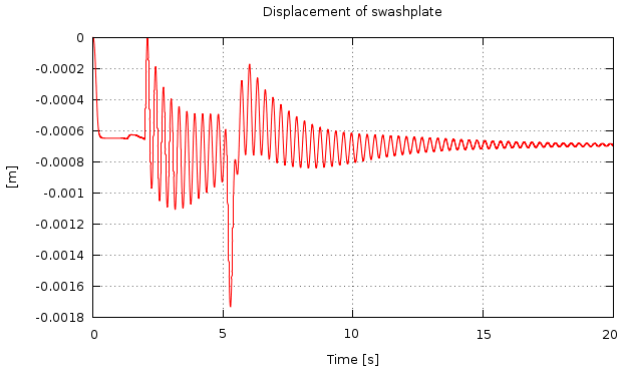

Figure 5.5: *Displacement of swashplate*

5.3 Double perturbation of collective lever

In the second test on the helicopter complete a double perturbation, still imposed by muscle, was uilizzata on the command of the collective order to excite different frequencies with respect to the previous case.

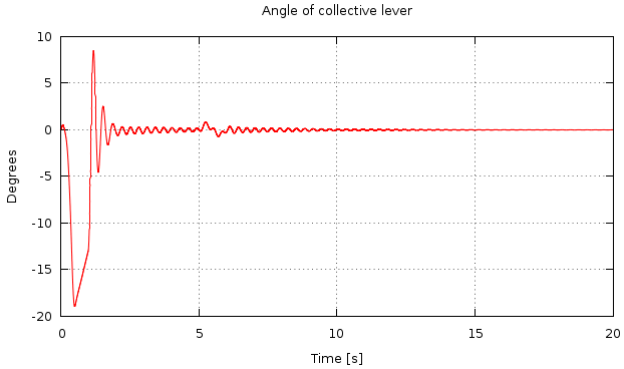

Figure 5.6: *Angle of collective lever*

Double perturbation means a movement with rotation of the lever upwards immediately followed by one opposite that harbors the lever in a specular position but negative, and finally a return of the lever to its initial position. To do this, it was necessary to give a sinusoidal law to muscle activations.

The figure 5.6 shows the time history of the command of the collective. From the graph of note as the angle of the lever to 5 seconds beginning to rotate upwards and then downwards following a sine wave. The movement ends as said with the command in its initial position.
The following graphs show the vertical position of the helicopter (Figure 5.7), which reflects the command imposed, the vertical acceleration of the center of gravity and finally the movement of the swash plate.

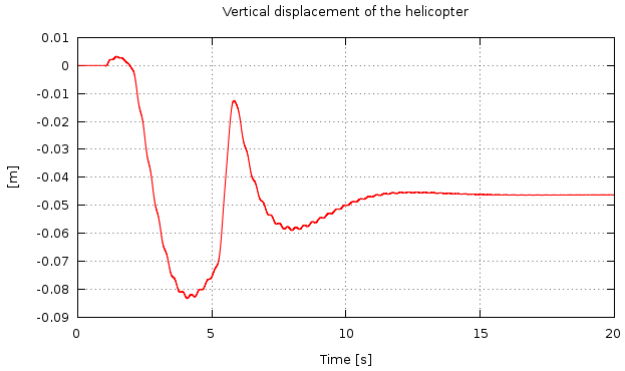

Figure 5.7: *Vertical displacement of the center of gravity of rotorcraft*

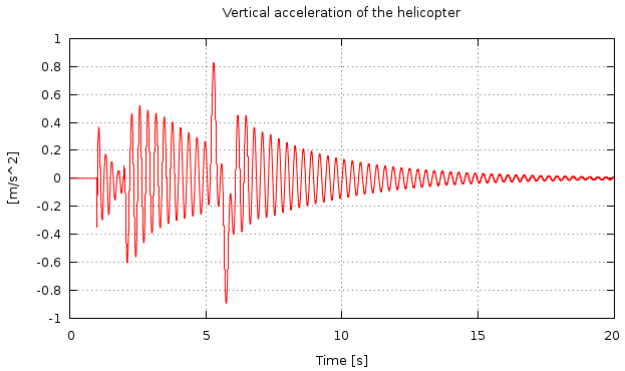

Figure 5.8: *Vertical acceleration of helicopter*

As mentioned previously, the swash plate goes down when the blades increase their angle.

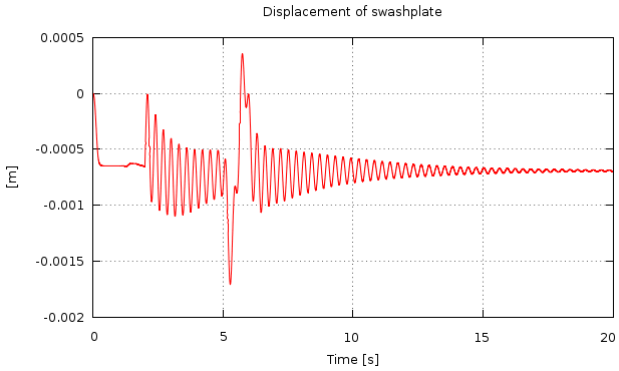

Figure 5.9: *Displacement of swashplate*

Chapter 6

Conclusions and future developments

During this thesis, the evidence for an analysis of the system behavior helicopter pilot subjected to various types of external disturbances have been developed successfully. The corresponding frequency responses were obtained and it was possible to compare them, with good results, with some evidence already available in the literature.
It was also developed a control system via activation of the arm muscle which allows movement under appropriate input.
This was inserted into a complete model of helicopter in order to simulate its behavior in an operational environment.
There are many possible future developments that might refine and expand the pilot model presented in this paper.
The first problem that must be solved, and that it is clear from the previous chapters is the lack of a link between the two arms, namely the torso. The current model is structured as if the seat belts fit together perfectly the shoulders of the pilot preventing any movement. This is obviously not possible in reality and therefore the presence of the torso and of a model of belts could make accessible these movements that otherwise would be lost. Above all, this addition would return to the two arms that dependence that one has on the other which is now entirely absent. In fact, right now they are acting like two completely separate entities and their simultaneous presence during a test is wholly irrelevant to the results.
With regard to the model helicopter, this can be developed by adding the control system of the cyclic and the respective arm inside the control cabin.

Bibliography

[1] A. Zanoni, *Estimation of the dependence of upper limb's bio-mechanical impedance on muscular activation using inverse dynamics* (2011),

[2] A. Zanoni, P. Masarati, G. Quaranta, *Upper limb mechanical impedance variability estimation by inverse dynamics and torque-less activation modes* (2011),

[3] S. Stroeve. *Impedance characteristics of a neuromusculoskeletal model of the human arm I. Posture control*

[4] Pavel, Malecki, DangVu, Masarati, Quaranta, Gennaretti, Jump, Smaili, Ionita, Zaicek, *Aircraft and Rotorcraft Pilot Coupling: a survey of recent research activities within the European project ARISTOTEL* (2011),

[5] D. T. McRuer, *Pilot-induced oscillations and human dynamic behavior* (1995),

[6] E. Pennesrtí, *Virtual musculo-skeletal model for the biomechanical analysis of the upper limb* (2006),

[7] V. Zatsiorsky *Kinematics of human motion* (1995),

[8] W. G. Bousman, C. Young, F. Toulmay, N. E. Gilbert, R. C. Strawn, J. V. Miller, T. H. Maier, M. Costes, P. Beaumier *A comparison of lifting-line and CFD methods with flight test data from a research Puma helicopter* (1996),

[9] John R. Mayo *The involuntary participation of a human pilot in a helicopter collective control loop* (1989),

[10] G. D. Padfield *Helicopter flight dynamics: the theory and application of flying qualities and simulation modeling* (1996),

[11] P. Masarati, G. Quaranta, M,Gennaretti, J. Serafini *An investigation of aeroelastic rotorcraft-pilot interaction* (2011),

[12] P. Masarati, G. Quaranta, M,Gennaretti, J. Serafini *Aeroservoelastic analysis of rotorcraft-pilot interaction by coupled bem-multybody solvers* (2010),

[13] P. Masarati, G. Quaranta, M,Gennaretti, J. Serafini *Aeroservoelastic Analysis of Rotorcraft-Pilot Coupling: a Parametric Study* (2010)